Wave-packet dynamics and photoionization in the Coulomb potential

Richard Dehnen
Fakultät für Physik, Albert-Ludwigs-Universität, 79104 Freiburg im Breisgau, Germany

Volker Engel
Institut für Physikalische Chemie, Universität Würzburg, 97070 Würzburg, Germany

(Received 13 April 1995)

We study the dynamics of radial wave packets in the singular Coulomb potential by solving the time-dependent Schrödinger equation numerically. A propagation scheme involving fast-Fourier transforms is used. We concentrate on the simple radial motion of the hydrogen atom to test the numerical method. In particular, we calculate the dynamics under the influence of a strong laser pulse and document how above-threshold-ionization peaks can be interpreted in terms of momentum-space wave functions. The results are compared to those obtained from a calculation that uses a soft core potential.

PACS number(s): 32.80.Rm, 32.80.Fb

I. INTRODUCTION

Numerous studies on the model problem of a one-dimensional atom interacting with a high intensity laser pulse can be found in the literature. For reviews of different approaches see the papers of Eberly and co-workers [1–4] and the references cited therein. Some of the most recent publications on this matter are listed in Refs. [5–8]. In most of the numerical studies a one-dimensional hydrogen atom is treated but the singular Coulomb potential is replaced by different kinds of "soft-core" potentials [3]. The reason for this is clear since any singularity introduces numerical instabilities. Obviously, one way to avoid these difficulties is to expand the time-dependent wave function in a basis of eigenfunctions of the unperturbed system. However this approach is not efficient if Rydberg or continuum states are excited since convergence with respect to the basis set expansion is hard to obtain. This is the case we study in the present paper. Another possibility is to artificially cut the singular potential at a finite distance and calculate the quantities of interest as a function of the cut-off parameter, hoping that convergence can be achieved. In this paper we want to pursue another approach: we solve the time-dependent Schrödinger equation directly on a grid and force the wave function to be zero at the origin so that the potential operator acting on the function remains finite. This idea was introduced by Hermann and Fleck in connection with wave-packet propagation in spherical coordinates [9]. Our intention is to present a method which is numerically stable, easily implemented, and can be efficiently used to treat Coulomb problems with attractive potentials. Furthermore it can be extended to electronic problems in higher dimensions [10].

After a description of our numerical scheme in Sec. II we will apply it to the radial hydrogen atom with zero angular momentum interacting with intense laser pulses (Sec. III). In addition, the results are compared to a calculation with a soft-core potential. Section IV contains a summary of the paper.

II. PROPAGATION SCHEME

We are interested in the solution of the time-dependent Schrödinger equation (atomic units are used throughout)

$$i\frac{\partial}{\partial t}\varphi = \{H_0 + H'(r,t)\}\varphi, \tag{1}$$

where

$$H_0 = -\frac{1}{2}\frac{1}{r^2}\frac{d}{dr}r^2\frac{d}{dr} - \frac{1}{r} \tag{2}$$

is the Hamiltonian for the radial motion of the hydrogen atom with zero angular momentum. We assume that the position of the nucleus coincides with the center of mass of the system. The perturbation in our model system is of the form

$$H'(r,t) = rE_0 f(t)\sin(\omega t), \tag{3}$$

which is the energy of an (isotropic) dipole in a homogeneous electric field of strength E_0 and energy ω. By treating the electric field as classical and independent of r, neither spontaneous emission nor laser focus effects are included here. $f(t)$ describes the envelope function of the light pulse. Note that r is a radial coordinate and thus assumes only positive values. This is an essential difference to other one-dimensional models (such as the soft-core model) which use a coordinate defined on the whole real axis. Thus in our model the electron dynamics is restricted to radial motion only, i.e., we investigate the motion of a sphere.

Another wave function is introduced by

$$\psi(r) = r\varphi(r). \tag{4}$$

The corresponding Hamiltonian which acts on this "reduced" function is

$$H(r,t) = -\frac{1}{2}\frac{d^2}{dr^2} - \frac{1}{r} + H'(r,t). \tag{5}$$

The definition (4) ensures that the wave function ψ is zero

at the origin. The time propagation is carried through in the Schrödinger representation approximating the time-evolution operator by short-time propagators. Therefore the propagation time t is divided into small increments Δt, so that the perturbation $H'(t)$ can be regarded as constant during the propagation interval Δt [11]. Then the wave function at time $t+\Delta t$ is

$$\psi(t+\Delta t) = U(\Delta t)\psi(t) = e^{-i\{H_0+H'(t')\}\Delta t}\psi(t), \quad (6)$$

where we have approximated H' by its value at the time $t' = t + \frac{\Delta t}{2}$. This ensures correct time ordering in the time-evolution operator. The numerical problem is to evaluate the action of the short-time propagator on the wave function. This is done with the "split-operator technique" [12] which approximates $U(\Delta t)$ as

$$U(\Delta t) = e^{-i(H_0+H')\Delta t} \sim e^{-i(-\frac{1}{r}+H')\frac{\Delta t}{2}} \times e^{-i(-\frac{1}{2}\frac{d^2}{dr^2})\Delta t} e^{-i(-\frac{1}{r}+H')\frac{\Delta t}{2}}. \quad (7)$$

This expression is correct up to second order in Δt but higher-order corrections can be obtained [13].

The wave function is represented on a spatial grid, hence the exponential parts of the short-time propagator (7) which depend on the radial coordinate r are evaluated by multiplication of the spatial wave function with the respective phase factors. The part of the propagator which contains the kinetic energy is evaluated in the same way by multiplication in momentum space. To do so, the wave function has to be transformed back and forth between coordinate and momentum space. This is efficiently done by fast-Fourier transforms.

In our propagation we use sine transforms which automatically ensure that the wave function has the right boundary condition at r=0. Also, we have to choose the coordinate grid large enough so that the wave function does not reach the grid boundary at large distances since, if this happens, the function is no longer periodic and reflections occur at the boundary. If we are not interested in the parts of the total function which are located at large distances we might remove them by use of an optical potential which has to be chosen carefully to avoid boundary reflections [14].

For the Coulomb problem we typically use grid lengths of 350 up to 1100 a.u. and a number of grid points between 4092 and 16 384. The choice of the time step used in our short-time propagator depends critically on the choice of the spatial grid. If, for a given grid length, the number of points N is increased, there will be grid points closer to zero and thus a larger negative value of the potential enters into the numerical calculation. This diminishes the accuracy of the split-operator approximation [15]. In our case we used a time step of about 10^{-4} a.u. Note that the electron dynamics determines the choice of Δt and not the approximation to replace the time-dependent perturbation $H'(t)$ by its value at the fixed time $t' = t + \frac{\Delta t}{2}$ during the short-time propagation. This follows from the fact that for our choice of parameters the temporal variation of the field is much slower than the dynamics determined by the Hamiltonian H_0.

III. RESULTS

As a first test of the method outlined above, we solved the eigenvalue problem of H_0 by using complex time propagation [16] of an initial Gaussian wave packet, i.e., taking e^{-sH_0} as propagator, where s is real and positive. Since this propagator is no longer unitary the wave packet asymptotically "relaxes" to the ground state of H_0. Higher states can be obtained by substracting the numerically obtained ground state from the initial wave packet. Another propagation yields the first excited state and so forth. We achieved accurate energies and wave functions [15] which increased our faith in the method. A similar method was applied recently to calculate the ground-state energies of s-state helium and H^- [10].

A. One-photon ionization

Next we studied the interaction of the system with a short and intense laser pulse. We chose a pulse envelope of the form

$$f(t) = \sin^2\left\{\frac{\pi t}{T}\right\} \quad (8)$$

and a field strength of E_0=0.7 a.u. The wave function at t=0 corresponded to the hydrogen s state $\psi(0) = re^{-r}$. An energy of ω=1.0 a.u. was used in a first calculation to investigate the case in which one-photon ionization occurs. The propagation time was $T = 20\pi$, i.e., ten optical cycles of the electric field. This laser parameters are, of course, fairly unrealistic concerning a real experimental arrangement. The choice was motivated by our intention to test the numerical method and to concentrate, for now, on the process of direct ionization.

Figure 1 shows the radial wave function during the interaction of the electric field with the model atom. After about three cycles of the laser field the wave packet has split into two parts. A further split into even more fractions is observed for longer times. The single packets move on average to larger distances, and when the field is turned off the single parts approach the asymptotic region with constant but different velocity. A similar behavior was found in a one-dimensional study by Schwengelbeck and Faisal [8]. These authors used the mean velocity of the separate packets to extract the kinetic energy and relate this to above-threshold-ionization (ATI) peaks. Since our calculation employs the coordinate- as well as the momentum space representation of the wave function at every time step, we might as well follow the dynamics of the momentum-space wave function during the time the field interacts with our one-dimensional model atom. The probability density $|\psi(p,t)|^2$ is plotted in Fig. 2. Starting from a symmetrical distribution around p=0 initially, it can be seen that during the time evolution the distribution shifts to purely positive momenta. Several peaks can be distinguished which oscillate around different mean momenta. When the pulse is switched off the momentum distribution remains unchanged which is characteristic for the motion of a free wave packet. We see that already after six cycles the momentum-space wave packet has split into different

parts which do not overlap. The single parts oscillate with the period of the electric field. This periodic motion represents acceleration and deceleration of the electrons within the statistical ensemble. The mean momentum of the single packets at the time when the field is turned off can be calculated also from the linear asymptotic motion of the fractional packets in Fig. 1 [8].

Figure 3 displays the probability distribution $|\psi(p,t)|^2$ at the time T, when the pulse is switched off, plotted versus the kinetic energy $E_p = \frac{p^2}{2}$. Calculations for an interaction time of 10 and 20 optical cycles are shown, respectively. The curves were normalized to each other at the maximum of the first peak. In both cases the ionization probability is almost equal to one. Four single peaks are found which are separated by the laser energy ω. We associate this maxima with above-threshold-ionization peaks. Although we have not projected on the correct Coulomb continuum functions but on plane waves the main appearance of the peaks is the same. It is interesting to note that, if the laser pulse interacts for 20 instead of 10 optical cycles with the model atom, the ratio of the peak maxima does practically not change. This confirms the observation discussed in connection with Fig. 2 that the overall ATI structure, which is reflected in the momentum-state wave function, already exists after only a short interaction time. The reason for this is that a direct bound-to-continuum transition is excited. No states other than the initial bound state are essentially populated: since the prepared wave packet moves outward towards larger distance a stimulated emission process is rather unlikely because the laser energy is off resonance by a large amount. It can be seen in Fig. 1 that most of the spatial electronic wave function moves far away from the nucleus and thus is in a region where further photon absorption is unlikely. We obtain an ionization probability of $\simeq$97.2% and a probability of finding the electron in the initial ground state at the end of the pulse of $\simeq$2.8%.

B. Three-photon ionization

The situation where the laser energy is such that three photons are needed for ionization is much more complicated than the one-photon ionization process discussed in the last subsection. This is due to the excitation of a coherent superpostion of Rydberg states, i.e., a Rydberg wave packet [17, 18]. We have seen in the last subsection that the wave function splits in several parts which oscillate with the period of the electric field. The underlying dynamics of this oscillations is the classical "quiver" motion of a free electron in an electric field. The corresponding equation of motion can be integrated analytically for the form of the electric field employed in our model [Eqs.

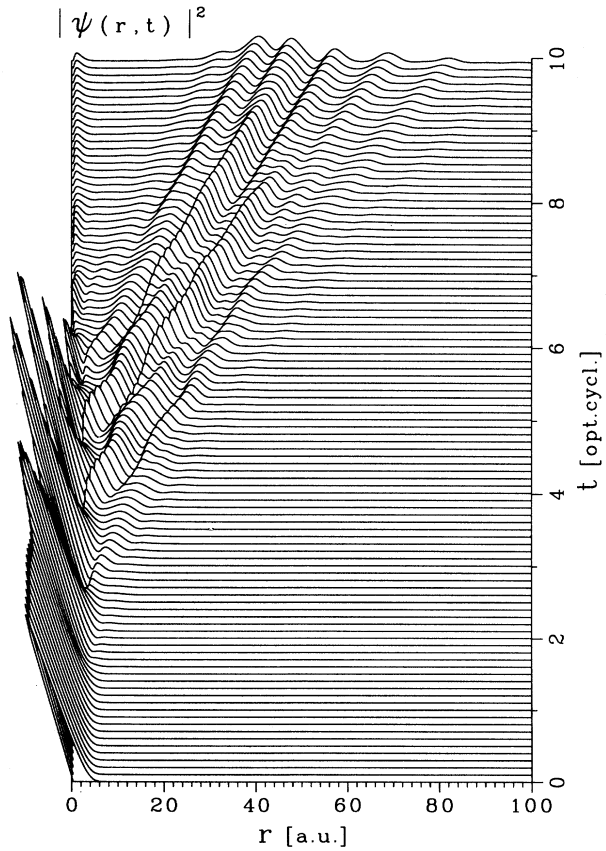

FIG. 1. Probability density in coordinate space: the time evolution is displayed for the case of a $\sin^2$ pulse with peak energy of 1 a.u. and a length of ten optical cycles.

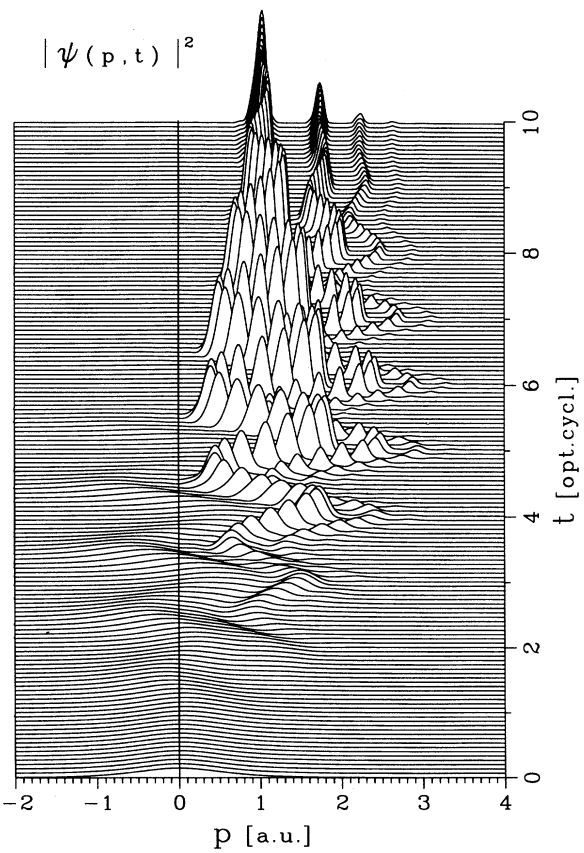

FIG. 2. Probability density in momentum space: the wave functions were obtained in the same calculation as the coordinate wave functions displayed in Fig. 1.

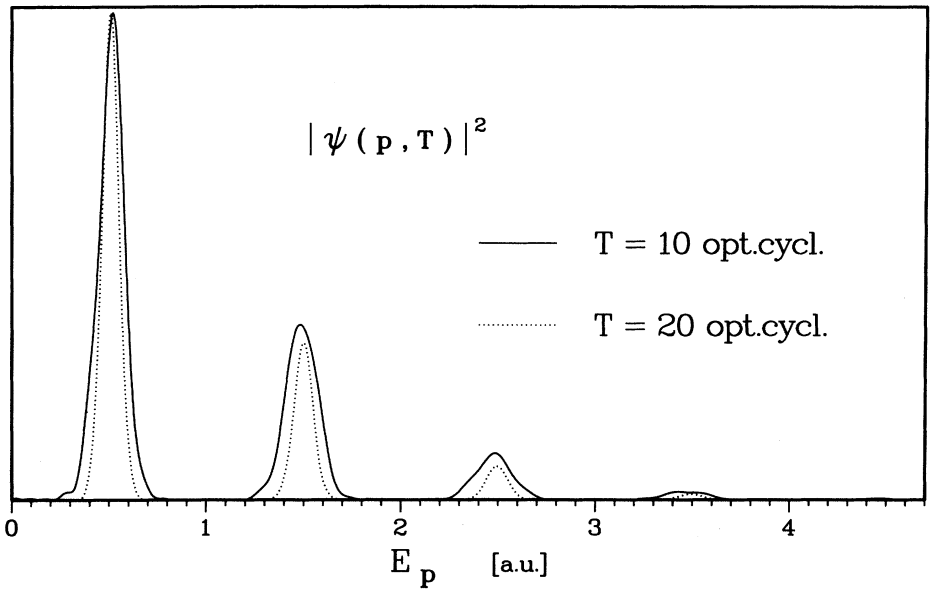

FIG. 3. Momentum distribution of the wave function at the end $t = T$ of the laser pulse plotted versus the kinetic energy. Results are displayed for pulses of 10 and 20 optical cycles length, as indicated.

(3) and (8)]. We use the initial condition p_0^{cl}=0 for the classical momentum since the momentum distribution of the initial quantum state is peaked around zero and furthermore the electric field envelope is exactly equal to zero at $t = 0$. The solution is

$$p_{cl}(t) = \frac{E_0}{4}\left(\frac{2\cos(\omega t)}{\omega} - \frac{\cos[(\omega+2\Omega)t]}{\omega+2\Omega} - \frac{\cos[(\omega-2\Omega)t]}{\omega-2\Omega} + \frac{8\Omega^2}{\omega(\omega^2-4\Omega^2)}\right), \quad (9)$$

where $\Omega = \frac{\pi}{T}$ [see Eq. (8)]. Since this classical dynamics does not yield further insight and makes it hardly possible to follow the formation of the fractional ATI wave packets during the pulse we substract it from the momentum-space wave packet to obtain the shifted wave function:

$$\psi'(p,t) = \psi(p - p_{cl}(t), t). \quad (10)$$

It should be noted that the continuum part of the wave function $\psi'(t)$, which is (at least approximately) the wave function of a free electron, does not move in momentum space. This is in contrast to the linear combination of bound states produced by the excitation process, which moves in the Coulomb potential and thus does not behave like a free electron. In the calculation we chose an energy of ω =0.23 a.u. and a field strength of E_0=0.7 a.u. Figure 4(a) displays the function for a 10-cycle pulse. For comparison the wave function obtained in the one-photon ionization process dicussed above is shown in Fig. 4(b). In both cases we observe the splitting of the wave function. The function for three-photon ionization looks almost stationary after about three cycles. This shows that at this time the ionization probability is nearly equal to one. It is possible to distinguish between three kinds of structures in the wave function. The maxima which are separated by the photon energy can be identified as the ATI peaks. As in the case of the one-photon ionization (see Fig. 2) almost all ATI peaks appear already after four optical cycles and do not change significantly from then on. The separation between them diminishes with increasing momentum since the energy depends quadratically on the momentum. After about five cycles additional smaller peaks appear. These sidebands are due to the envelope function of the short pulse. Furthermore the figure shows a broader structure with a minimum at $p - p_{cl} \simeq 2.7$ a.u. which is superimposed on the peaks we just discussed. A similar minimum has been seen in other calculations [1, 4, 19] but the physical meaning is not yet understood. There might be a relation to a theory of photoionization, originating in the work of Keldysh [20, 1, 21]. It is not clear to us if this theory applies to our case of short-pulse excitation. No attempt was made to modify the theory which would go far behind the purpose of this paper. We note, that the additional structure appears in a slightly different form for other envelope functions (e.g., a Gaussian profile or a square pulse) and disappears at lower intensities (see Fig. 3). We carefully checked our numerics and found the results to be converged with respect to the time step and the grid parameters.

Figure 5 shows part of the electron spectrum. The curve was obtained by successively substracting the bound states from the wave function $\psi(T)$ until convergence was obtained. The figure displays the momentum-space wave function calculated in this way plotted versus the energy $E_p = \frac{p^2}{2}$. A rich structure is encountered. Many of the peaks are separated by the photon energy thus are ATI peaks. Sidebands occur as well and the structures mentioned above are clearly visible.

IV. COMPARISON TO THE SOFT-CORE MODEL

Finally we want to compare our results to the case when the Coulomb potential is replaced by the soft-core potential

$$V(x) = -\frac{V_0}{\sqrt{1+x^2}}, \tag{11}$$

where the variable x now takes positive and negative values. V_0 was chosen to be 0.779 532 a.u. to give the same binding energy as the Coulomb potential. This model potential was extensively studied by Eberly and co-workers [1, 2]. Figure 6 shows the momentum-space wave function for a 10 cycle pulse of field strength E_0=0.7 a.u. and an energy of ω=1 a.u. The initial wave function was the numerically calculated ground state. Again we notice the oscillation with the optical cycle. In contrast to the Coulomb case (Fig. 2) the momentum distribution here oscillates around zero momentum during the whole excitation process. One observes ATI peaks for negative as well as positive momenta. This is due to the soft-core potential which allows electronic motion in positive and negative directions and has only a finite well depth. On the contrary, in our radial model an incoming electron is reflected as soon as it approaches the nucleus. Since in the inner potential region ionization occurs with high probability the negative momentum parts belonging to

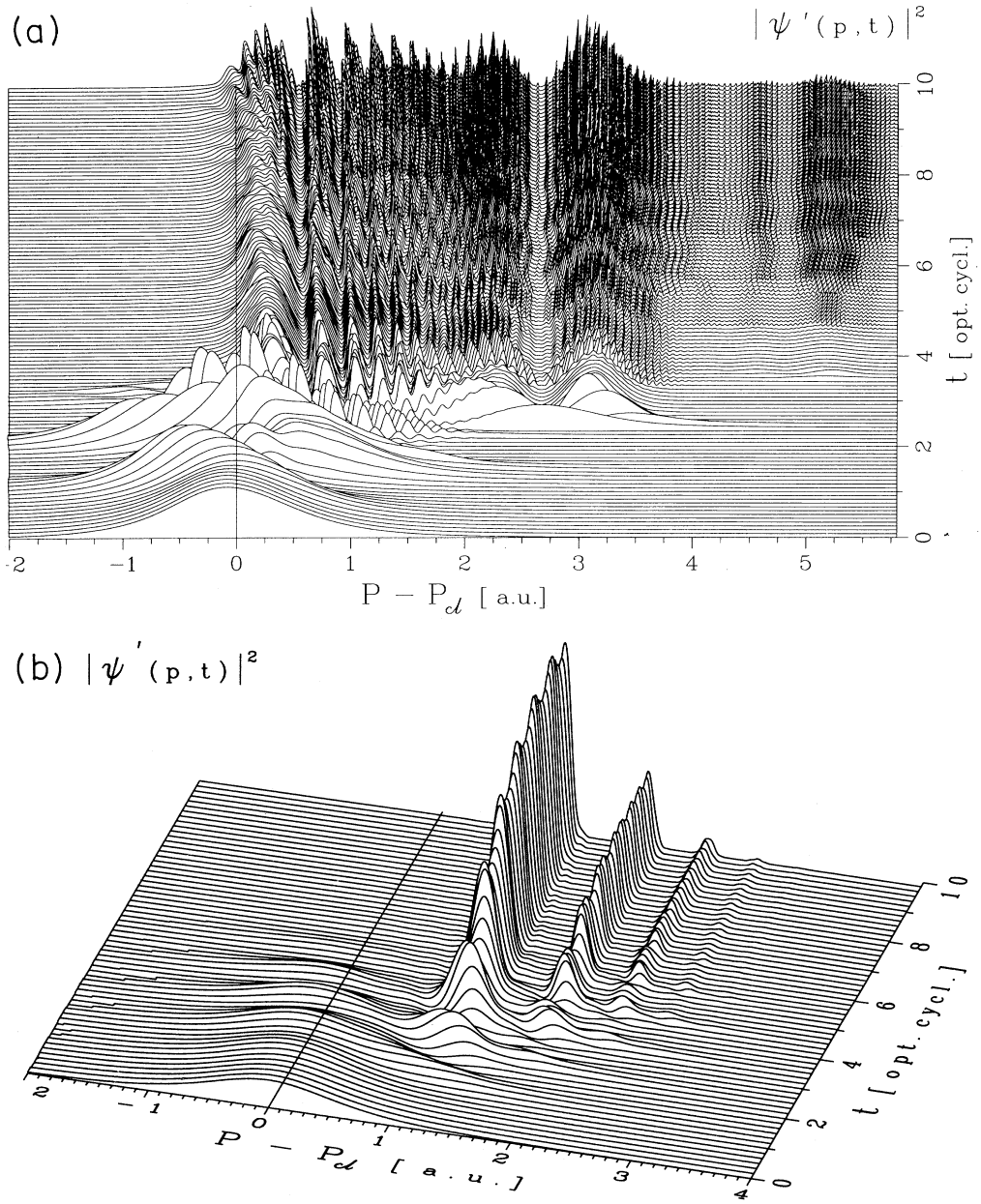

FIG. 4. (a) Momentum-space dynamics for the case of three-photon ionization (ω = 0.23 a.u.). The classical motion of a free electron in an electric field is substracted as described in the text. (b) Same as (a) but for one-photon ionization (ω = 1.0 a.u.).

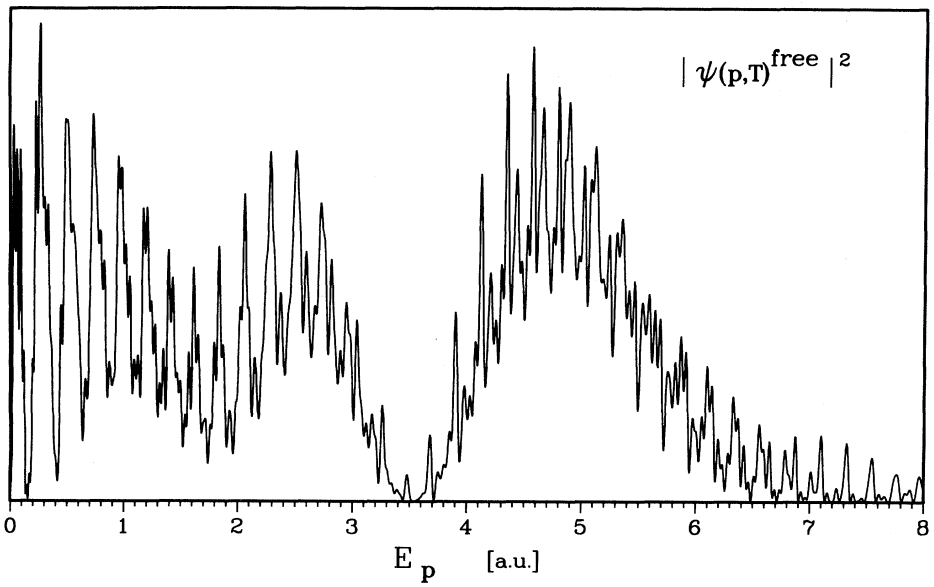

FIG. 5. Momentum distribution of the wave function at the end of the laser pulse for the case of three-photon excitation plotted as a function of the kinetic energy up to 8 a.u. The bound state part of the total wave function was substracted before calculating the distribution.

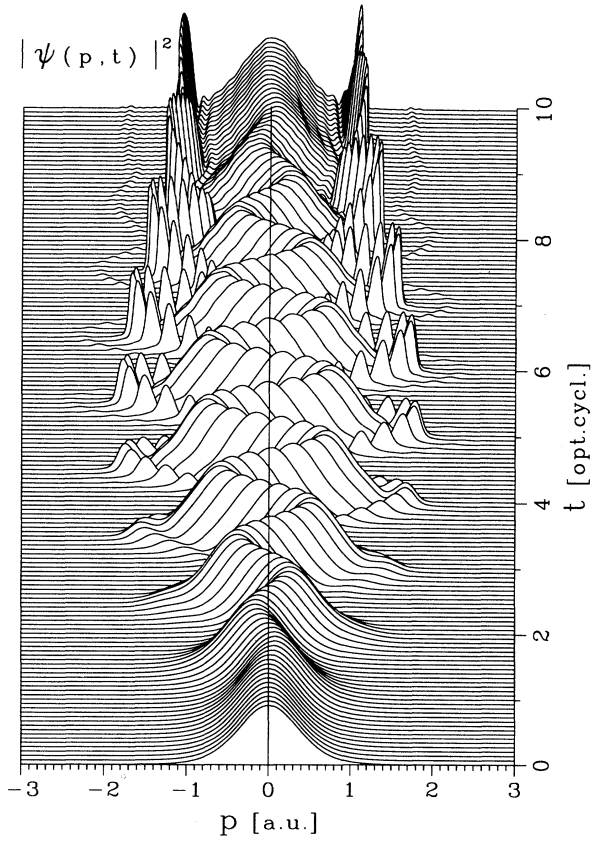

FIG. 6. Momentum-space probability distribution for laser excitation within the soft-core model. The time evolution is displayed for the case of one-photon ionization ($\omega = 1$ a.u.).

bound states disappear faster than in the case where a soft-core potential is used.

Note that the wave function has not to be symmetrical with respect to the coordinate origin. From the figure it is obvious that in the present case the ionization yield is much lower compared to the case of the radial Coulomb model: the final wave function has a large probability amplitude near zero momentum which belongs to bound-state wave functions. In fact, about 75% of the wave function remains in the initial ground state. The same was found in the case where results from calculations with *hard*- and *soft*-core potentials were compared [8]. If a projection on plane waves is performed only one ATI peak of substantial magnitude is present.

V. SUMMARY

We have presented a numerical method which allows for the efficient and stable propagation of an electronic wave packet. The method was applied to the one-dimensional radial hydrogen atom in an intense laser field.

For the case of one-photon ionization the time evolution of the momentum-space wave function documents the formation and dynamics of ATI peaks. If several photons are required for ionization, the situation becomes more complicated due to the temporal excitation of higher bound states of the electron. Besides high-order ATI peaks which are separated by the photon energy and further sidebands, a pronounced structure is encountered in the electron spectrum. We were not yet able to give a consistent interpretation of this effect, but work is in progress.

Comparison between the model of the radial hydro-

gen atom with the Coulomb potential and another model which uses a soft-core potential shows that in the latter the ionization rate is much lower. In the soft-core case only one ATI peak is encountered for the employed intensity whereas in our model higher order peaks occur.

ACKNOWLEDGMENTS

Financial support by the DFG within the SFB 276 is acknowledged. We thank G. Alber, C. Meier, and J.-M. Rost for helpful discussions.

[1] J. Javanainen, J.H. Eberly, and Q. Su, Phys. Rev. A **38**, 3430 (1988).
[2] Q. Su and J.H. Eberly, J. Opt. Soc. Am. B **7**, 564 (1990).
[3] J.H. Eberly, J. Javanainen, and K. Rzazewski, Phys. Rep. **204**, 331 (1991).
[4] J.H. Eberly, R. Grobe, C.K. Law, and Q. Su, in *Atoms in Strong Fields*, edited by M. Gavrila (Academic Press, San Diego, 1992).
[5] L. Roso-Franco, A. Sanpera, M.Ll. Pons, and L. Plaja, Phys. Rev. A **44**, 4652 (1991).
[6] Y. Gontier and M. Trahin, Phys. Rev. A **46**, 1488 (1992); C. Cerjan and R. Kosloff, *ibid.* **47**, 1852 (1993); X. Tang and S. Basile, *ibid.* **44**, R1454 (1991).
[7] Q. Chen and I.B. Bernstein, Phys. Rev. A **47**, 4099 (1993).
[8] U. Schwengelbeck and F.H.M. Faisal, Phys. Rev. A **50**, 632 (1994).
[9] M.R. Hermann and J.A. Fleck, Jr., Phys. Rev. A **38**, 6000 (1988).
[10] L. Zhang, J. Feagin, V. Engel, and A. Nakano, Phys. Rev. A **49**, 3457 (1994).
[11] R.W. Heather, Comput. Phys. Commun. **63**, 446 (1991).
[12] M.D. Feit and J.A. Fleck, Jr., J. Chem. Phys. **80**, 2578 (1984); J.A. Fleck, Jr., J.R. Morris, and M.D. Feit, Appl. Phys. **10**, 129 (1976).
[13] H. Yoshida, Phys. Lett. A **150**, 262 (1990); A.D. Bandrauk and H. Shen, Chem. Phys. Lett. **176**, 428 (1991).
[14] D. Neuhauser and M. Baer, J. Chem. Phys. **90**, 4351 (1989); D. Neuhauser, *ibid.* **95**, 4927 (1991).
[15] R. Dehnen, Diploma thesis, University of Freiburg, 1993 (unpublished).
[16] R. Kosloff and H. Tal-Ezer, Chem. Phys. Lett. **127**, 223 (1986).
[17] A. ten Wolde, L.D. Noordam, A. Lagerdijk, and H.B. van Linden van der Heuvel, Phys. Rev. A **40**, 485 (1989); J.A. Yeazell, M. Mallalieu, and C.R. Stroud, Phys. Rev. Lett. **64**, 2007 (1990); D.R. Meacher, P.E. Meyler, I.G. Hughes, and P. Ewart, J. Phys. B. **24**, L63 (1991).
[18] G. Alber, H. Ritsch, and P. Zoller, Phys. Rev. A **34**, 1058 (1986); G. Alber and P. Zoller, Phys. Rep. **199**, 231 (1991).
[19] R. Grobe and J.H. Eberly, Phys. Rev. A **48**, 4664 (1993).
[20] L.V. Keldysh, Zh. Eksp. Teor. Fiz **47**, 1945 (1964) [Sov. Phys. JETP **20**, 1307 (1965)].
[21] W. Becker, L. Davidovich, and J.K. McIver, Phys. Rev. A **49**, 1131 (1994).